HHS Public Access

Author manuscript

FASEB J. Author manuscript; available in PMC 2022 June 10.

Published in final edited form as:

FASEB J. 2022 May ; 36(5): e22286. doi:10.1096/fj.202101837R.

Epidermal growth factor deficiency predisposes to progressive renal disease

Alia M. Zeid[1], **Joseph O. Lamontagne**[1], **Hui Zhang**[1], **Alexander G. Marneros**[1,*]

[1]Cutaneous Biology Research Center, Department of Dermatology, Massachusetts General Hospital and Harvard Medical School, Charlestown, MA, 02129, USA

Abstract

Epidermal growth factor (EGF) is produced in the kidney by thick ascending limbs (TALs) and distal convoluted tubules (DCTs). Reduced urinary EGF levels have been associated with chronic kidney disease but it is not known whether physiological levels of EGF protect the kidney from progressive renal disease. Here, we show that EGF-deficient mice on a mixed genetic background had increased urinary microalbumin, and a subset of these mice developed severe progressive renal disease with azotemia that was not seen in WT or TGFα-deficient littermates with this mixed genetic background. These azotemic EGF-deficient mice developed crescentic glomerulonephritis linked to HB-EGF/EGFR hyperactivation in glomeruli, as well as attenuation of the proximal tubule brush border, DCT dilatation, and kidney fibrosis associated with renal β-catenin/mTOR hyperactivation. The observation of these severe renal pathologies only in a subset of EGF-deficient mice suggests that independent segregation of strain-specific modifier alleles contributes to the severity of the renal abnormalities that only manifest when EGF is lacking. These findings link the lack of EGF to renal pathologies in the adult mammalian kidney, in support of a role of physiological levels of EGF for maintaining the function of glomeruli, PTs, and DCTs. These observations suggest that diminished EGF levels predispose kidneys to progressive renal disease.

Keywords

epidermal; growth; factor/kidney/renal; fibrosis/renal; failure/glomerulonephritis

INTRODUCTION

Epidermal growth factor (EGF) is expressed in the adult at high levels particularly in submandibular glands and thick ascending limbs (TALs) and distal convoluted tubules (DCTs) of the distal nephron in the kidney (1–4). The physiological function of EGF in the adult is not well understood, particularly because previous analyses of young adult EGF-deficient ($Egf^{-/-}$) mice did not identify major abnormalities (5). EGF is found as a

*Corresponding author: Alexander G. Marneros, MD/PhD, amarneros@mgh.harvard.edu.

AUTHOR CONTRIBUTIONS: Experimental procedures were performed by all authors. Data analysis, writing of the manuscript, and figure preparations were done by AGM.

CONFLICT OF INTEREST STATEMENT: The authors declare no conflicts of interests.

membrane-bound prepro-EGF precursor molecule that is released proteolytically to generate the 53-amino acid peptide hormone EGF. No EGF expression is detected in proximal tubules (PTs) in the kidney, but urinary EGF proteins line the apical PT membranes (1–3). EGF is present in urine at much higher concentrations than in serum, which suggests that a significant proportion of urinary EGF is derived from TALs/DCTs and not from glomerular filtration (6). This is also supported by mouse studies, which showed that a rapid increase in urinary EGF occurs mostly between day 6 and day 18 postnatally, which correlates with the onset of EGF expression in maturing TALs/DCTs (EGF is detected after postnatal day 3 [P3] and expression increases after P3) (2, 7). Moreover, urinary EGF levels correlated with intrarenal mRNA EGF levels (8). Notably, the concentration of urinary EGF declines with progressive age (9, 10). Lower baseline urinary EGF excretion has been associated with decreased renal function and chronic kidney disease (CKD) (8, 11). This raises the question of whether EGF production in the kidney helps maintain renal function and protects the kidney from CKD-like pathologies, such as renal fibrosis and inflammation, and whether the decline in EGF with aging increases the risk for CKD. However, whether physiological levels of EGF have indeed such a protective role for the adult kidney has not been assessed yet.

The EGF/EGF receptor (EGFR) family consists of different ligands and receptors. Single-cell RNA-Seq (scRNA-Seq) of adult mouse kidneys confirmed previous immunolabeling studies and showed that EGF is highly expressed specifically in TALs and DCTs (12). We also confirmed by immunolabeling for EGF that cytoplasmic EGF is detected only in TALs/DCTs in the adult mouse kidney and in no other nephron segments, with the onset of expression after postnatal day 3 with the maturation of nephron segments (2). Thus, EGF serves as a terminal differentiation marker of TALs/DCTs. The scRNA-Seq data also show that EGF is the main EGFR family ligand that is expressed at high levels in TALs/DCTs, whereas its family member TGFα is expressed in podocytes, thin limbs of Loop of Henle (LOH), and collecting ducts (CDs) (12). HB-EGF is expressed in PTs, thin limbs of LOH, and intercalated cells of cortical CDs, but not in podocytes (12). Betacellulin is expressed in CDs, whereas CTGF is expressed in podocytes and has been recently shown to act as an EGFR ligand as well. The EGF receptor family consists of EGFR (ErbB1), ErbB2, ErbB3, and ErbB4 that can homo- or heterodimerize (13). EGF binds specifically to EGFR (to either EGFR homodimers or EGFR/ErbB2 heterodimers). ScRNA-Seq did not detect high-level expression of EGFR in TAL/DCT cells but in cells of other nephron segments, whereas ErbB2 and ErbB4 are highly expressed in TALs, and ErbB3 mainly in CDs (12). However, earlier studies suggested that EGFR is expressed by TALs and DCTs as well (14).

The EGFR is normally expressed at the basolateral membrane in nephron epithelia, but under pathologic conditions, an apical mislocalization of the EGFR can occur, or tight junction abnormalities may allow urinary EGF to bind to basolateral EGFR. Notably, it has been shown that hyperactivation of EGFR signaling in glomeruli through aberrant overexpression of HB-EGF in podocytes leads to rapidly progressive glomerulonephritis with the formation of cellular crescents in glomeruli (multilayered accumulation of proliferating cells in Bowman’s space) and accumulation of T cells and macrophages in glomeruli (15). Cellular crescents are pathognomonic for inflammatory glomerulonephritis.

EGFR deficiency results in severe abnormalities that strongly depend on the genetic background of the mice: $Egfr^{-/-}$ mice on a CF-1 background had peri-implantation death due to degeneration of the inner cell mass, whereas EGFR deficiency on a 129/Sv background resulted in death at mid-gestation due to placental defects. $Egfr^{-/-}$ mice on a CD-1 background survived until 3 weeks after birth and showed abnormalities in skin, kidney, brain, liver, and gastrointestinal tract (16). These mice developed progressive cystic dilatation of CDs with flattened epithelial lining and increased BUN, consistent with a critical role of EGFR for CDs that normally highly express EGFR (12, 16). The findings suggest the presence of strain-specific genetic modifiers that have a major effect on EGFR-dependent phenotypes.

In contrast, the lack of a reported kidney phenotype in young adult mice lacking EGF raises the question as to the physiological relevance of EGF-dependent signaling for renal function in the adult and during aging (5). We also found that young adult $Egf^{-/-}$ mice (6-weeks-old) did not show major histological or functional abnormalities of their kidneys and had normal protein levels of TAL differentiation markers (NKCC2) and DCT differentiation markers (NCC, parvalbumin) (2). This raises the question of whether EGF has non-redundant functions in adult kidney physiology, and whether lack of EGF results in renal defects with age progression. Based on *in vitro* studies, it has been proposed that EGF promotes urinary Mg^{2+} uptake in DCTs, but $Egf^{-/-}$ mice had normal Mg^{2+} serum levels, demonstrating that EGF deficiency is not a critical regulator of Mg^{2+} homeostasis (4, 17). EGF has been shown to regulate sodium transport in the distal nephron via the sodium transporter ENaC, and chronic EGF treatment inhibited ENaC activity *in vitro* (18). Moreover, infusion of EGF decreased ENaC activity in CDs and attenuated salt-induced hypertension (13, 19). However, whether EGF-deficiency affects electrolyte homeostasis *in vivo* is not known.

Exogenous EGF administration reduced experimental acute kidney injury in a model of ischemia-reperfusion injury, suggesting that EGF may promote repair of tubular injury (20). Similarly, exogenous administration of EGF reduced CD cyst formation in a mouse model of autosomal recessive polycystic kidney disease (21). In contrast, distal nephron differentiation defects that lead to tubule dilatation in mice lacking KCTD1 were not prevented by a similar regimen of EGF administration (2). Importantly, these previous studies showed effects of exogenously administered EGF only *in vitro* or in animal models of kidney diseases, but no *in vivo* data has established a protective role of EGF under normal physiological conditions for kidney function in the adult or during aging. Thus, we analyzed here whether EGF deficiency affects kidney function and determined whether progressive age and genetic background have a major influence. As phenotypes in $Egfr^{-/-}$ mice were strongly dependent on the genetic background, we paid particular attention to whether there is a marked variability of a renal phenotype in these $Egf^{-/-}$ mice that may be explained by the heterogeneous genetic background due to effects of strain-specific modifier alleles. Our findings suggest that EGF promotes renal function in the adult, and its deficiency predisposes kidneys to progressive glomerulonephritis, renal fibrosis, and inflammation.

MATERIALS AND METHODS

Animals

The generation of $Egf^{-/-}$ mice and $Tgfa^{-/-}$ mice has previously been reported (5). We utilized $Egf^{-/WT}Tgfa^{-/WT}$ mice that were on a mixed genetic background to produce the following experimental groups: WT mice, $Egf^{-/-}$ mice, $Tgfa^{-/-}$ mice, and $Egf^{-/-}Tgfa^{-/WT}$ mice. These mice were obtained from MMRRC and showed a substantial degree of heterozygosity (Mouse Universal Genotyping Array [MUGA] showed that ~30% of the genome was heterozygous; C57bl6 and Sv129 mixed genetic background). Mouse serum BUN levels and chemistries were determined with a Dri-Chem7000 chemistry analyzer (Heska). Urine microalbumin was measured with a Siemens DCA Vantage analyzer. The exact number of mice for which urinary microalbumin, serum BUN levels, and serum chemistries were measured are indicated in Figures 1B, 1C, and S2.

Study Approval

For all animal studies, institutional approval was granted and international guidelines for the care and use of laboratory research animals were followed. ARRIVE (Animal Research: Reporting of In Vivo Experiments) guidelines for reporting animal studies were followed.

Immunolabeling of kidney sections and morphological kidney analyses

Kidneys of $Egf^{-/-}$ mice with increased BUN levels as well as age-matched WT and $Tgfa^{-/-}$ controls were assessed by histology and by immunolabeling. For morphological analysis of mouse kidneys, they were fixed in 4% paraformaldehyde. Kidneys were bisected and then processed and embedded in paraffin for histological analysis. H&E, PAS, and Trichrome stainings were performed according to standard protocols. The other kidney half was embedded in 30% sucrose and subsequently in OCT for immunolabeling experiments. For immunolabeling, 7μm kidney sections were permeabilized in 0.5% Triton X-100 and subsequently blocked with serum in which the secondary antibodies were raised. The following primary antibodies were used: rat anti-F4/80 (conjugated with Alexa647, BioLegend Cat# 123121, RRID:AB_893492), goat anti-Aqp2 (Santa Cruz Biotechnology Cat# sc-9882, RRID:AB_2289903), rabbit anti-NCC (Millipore Cat# AB3553, RRID:AB_571116), rabbit anti-NKCC2 (Cell Signaling Technologies Cat# 38436, RRID:AB_2799134), rabbit anti-parvalbumin (Abcam Cat# ab11427, RRID:AB_298032), goat anti-EGF (R&D Systems Cat# AF2028, RRID:AB_355111), Cy3-conjugated mouse monoclonal SMA (clone 1A4) (Sigma-Aldrich Cat# A2547, RRID:AB_476701) antibodies, rat anti-CD31 (BD Biosciences Cat# 550274, RRID:AB_393571), rabbit anti-cleaved caspase-3 (Asp175) (Cell Signaling Technology Cat# 9664, RRID:AB_2070042), rat anti-CD45 (BD Biosciences Cat# 550539, RRID:AB_2174426), rabbit anti-TFEB (Bethyl Cat# A303–672A, RRID:AB_11204598), rabbit anti HB-EGF (ABclonal Cat# A16365, RRID:AB_2760743), and rabbit anti phospho EGFR (Tyr1068) (D7A5) (Cell Signaling Technology Cat#3777, RRID:AB_2096270), and rat anti-CD3 (Abcam Cat# ab11089, RRID:AB_2889189). Phalloidin conjugated with Alexa647 (Thermo Fisher Scientific Cat# A22287, RRID:AB_2620155) was used for cytoskeletal staining at a dilution of 1:100. DAPI was used to stain nuclei (Thermo Fisher Scientific Cat# D3571, RRID:AB_2307445). Secondary Alexa-488/555/647 antibodies were used at a dilution of 1:200 (Thermo Fisher).

Lectins at a dilution of 1:100 were from Vector Laboratories: rhodamine-conjugated peanut agglutinin (PNA; Vector Laboratories Cat# RL-1072, RRID:AB_2336642) [epithelial staining of distal nephron epithelial cells; contiguous staining of PTs], fluorescein-conjugated Lotus Tetragonolobus Lectin (LTL; Vector Laboratories Cat# FL-1321, RRID:AB_2336559) [labels PTs].

For semithin sections, bisected kidneys were fixed in 1.25% paraformaldehyde and 2.5% glutaraldehyde in 0.1 M cacodylate buffer (pH 7.4). After postfixation in 4% osmium tetroxide, and dehydration steps, tissues were embedded in TAAB epon (Marivac Ltd.) and 1μm thin sections were used for toluidine blue staining and light microscopy.

Western blotting

Kidneys were lysed in NP40 lysis buffer (Life Technologies) with 1mM PMSF and protease inhibitor cocktail (Complete, Roche) using the Qiagen TissueLyser-II. After centrifugation, the protein concentrations in the supernatant were determined with a Bradford assay. Equal amounts of protein were loaded onto NuPage 4–12% Bis-Tris gels (Life Technologies) and blotted to nitrocellulose membranes. Equal protein loading was assessed using a rabbit polyclonal anti-β-actin antibody (Cell Signaling Technology Cat# 4970, RRID:AB_2223172). The following primary antibodies were used: antibodies against NKCC2 (38436, Cell Signaling Technology), NCC (Millipore Cat# AB3553, RRID:AB_571116), active β-catenin (non-phospho Ser33/37/Thr41) (Cell Signaling Technology Cat# 8814S, RRID:AB_11127203), phospho 4E-BP1 (Thr37/46) (Cell Signaling Technology Cat# 2855, RRID:AB_560835), p70 S6 kinase (Cell Signaling Technology Cat# 2708, RRID:AB_390722), rabbit anti-TFEB (Bethyl Cat# A303–672A, RRID:AB_11204598), and rabbit anti-Scl3a1 (Proteintech Cat# 16343–1-AP; RRID:AB_2239419). HRP-conjugated secondary antibodies were used and chemiluminescence signal was determined with the SuperSignal WestPico chemiluminescent substrate (Pierce). Band intensities were quantified with Image J.

Statistics

A Mann-Whitney test was used to calculate p-values. P-values <0.05 were considered to be statistically significant. P-values are indicated. All graphs show mean ± SEM.

Graphs and descriptive statistics (Figure S3) were obtained with Prism 9.3.1 (Graphpad).

Results

EGF deficiency does not affect nephrogenesis or kidney function in young adult mice

Analysis of scRNA-Seq data of adult mouse kidneys shows that EGF is expressed in the kidney at high levels only in TALs and DCTs, while other EGF family ligands do not show strong expression in TALs/DCTs (Figure S1) (12). This is consistent with our immunolabeling data that detected cytoplasmic EGF only in TALs/DCTs of adult kidneys (2, 17). In contrast, the scRNA-Seq data show no high-level expression of the EGFR in TALs/DCTs, which is required for EGF-mediated signaling, whereas the EGFR family

members ErbB2 and ErbB4 are highly expressed in TALs (Figure S1) (12). Notably, we found that EGF expression in mouse kidneys postnatally occurs after P3 (2).

To determine the relevance of physiological levels of EGF for kidney function we assessed $Egf^{-/-}$ mice, in which we confirmed the complete absence of EGF protein by lack of EGF immunolabeling in their kidneys (2, 5, 17). We utilized $Egf^{-/WT}Tgfa^{-/WT}$ mice on a mixed genetic background to produce the following experimental groups: WT mice, $Egf^{-/-}$ mice, $Tgfa^{-/-}$ mice, and $Egf^{-/-}Tgfa^{-/WT}$ mice. These mice showed a substantial degree of heterozygosity (Mouse Universal Genotyping Array [MUGA] showed that ~30% of the genome was heterozygous; C57bl/6J and Sv129P2/OlaHsd mixed genetic background). All these mouse groups were viable and were observed at the expected Mendelian ratio when assessed at 4 weeks of age (Figure 1A). Histopathologic analysis of kidneys in young adults of these experimental groups displayed no major morphologic abnormalities. Analysis of BUN levels in these groups of mice at 1 month of age showed no major abnormalities as well (Figure 1B). Moreover, levels of serum electrolytes, calcium, phosphate, albumin, and total protein were normal in 2–4 months-old as well as 9–12 months-old EGF-deficient mice (Figure S2). EGF deficiency did not affect protein levels of the PT differentiation marker Slc3a1 or the DCT differentiation marker NCC in whole kidney lysates of 1-months-old adult mice that showed no azotemia (Figure 2). Similarly, adult TGFα-deficient mice showed no reduction in these differentiation markers as well (Figure 2). Thus, neither EGF nor TGFα is critical for normal kidney development and renal function in young adult mice.

Renal abnormalities in a subset of EGF-deficient mice

The observation of decreased urinary EGF levels in patients with CKD raises the question of whether a lack of physiological levels of EGF predisposes to an impairment of renal function in the adult. To test for such a potential protective role of physiological levels of EGF for kidney function, we first measured BUN levels in different age groups of $Egf^{-/-}$ mice, $Egf^{-/-}Tgfa^{-/WT}$ mice, $Tgfa^{-/-}$ and WT littermates up to 12 months of age, as a high increase in BUN correlates with severe renal dysfunction. Across all age groups, we measured BUN levels in 93 WT mice and 71 $Tgfa^{-/-}$ mice. All of these mice had normal BUN levels (Figure 1B). In contrast, a subset of both $Egf^{-/-}$ (5.8%; 8 of 137 mice) and $Egf^{-/-}Tgfa^{-/WT}$ (14.1%; 10 of 71 mice) mice developed renal impairment with an increase in BUN levels (BUN levels that were higher than the highest measurement in the age-matched WT or $Tgfa^{-/-}$ control groups) (Figure 1B; descriptive statistics shown in Figure S3). In comparison to the control groups (WT and $Tgfa^{-/-}$ mice; 164 mice total), 18 of 208 mice in the $Egf^{-/-}$ and $Egf^{-/-}Tgfa^{-/WT}$ groups had an increase in BUN levels, many of which were very high and were accompanied by premature death due to renal failure.

As the high increase in BUN may manifest only with more advanced renal disease, we tested whether EGF-deficient mice that do not have yet a high increase in BUN levels may already have more subtle renal abnormalities, which may be reflected in an increase in urinary microalbumin (a sensitive marker of renal defects). Indeed, we observed in more than 50% of 10–13 months-old $Egf^{-/-}$ mice, which we selected out of those mice that did not show an increase in BUN yet, a significant relative increase in urinary microalbumin compared to age-matched WT or $Tgfa^{-/-}$ groups (Figure 1C). This suggests that underlying

renal abnormalities occur in most EGF-deficient mice even when their BUN levels are not increased yet. These findings are consistent with a high degree of variability in the renal phenotype of adult mice lacking EGF, whereas none of the mice in the large control groups did show these renal abnormalities. The data suggest a contributory but not essential role of EGF for maintaining renal function in the adult mammalian kidney.

Severe crescentic glomerulonephritis, renal fibrosis, and defects in PTs and DCTs in azotemic adult $Egf^{-/-}$ mice

Histomorphologic analysis of kidneys of those $Egf^{-/-}$ and $Egf^{-/-}Tgfa^{-/WT}$ mice with high BUN levels (azotemia) demonstrated severe renal abnormalities (Figures 3A–3D). Tubular dilatation was particularly observed for cortical distal nephron tubules (Figure 3A). Glomeruli showed glomerulosclerosis with an increased mesangial matrix, a lobular glomerular pattern, and crescents in Bowman's space (Figure 3A). Trichrome staining identified areas of fibrosis within glomeruli (glomerulosclerosis), as well as in tubulointerstitial areas of the renal cortex (Figure 3A). Wedge-shaped areas extending from the renal cortex to the medulla with atrophic tubules with diminished lumen were present (Figure 3B). PAS staining highlighted cellular crescents in Bowman's space, and PAS^{+} material was observed in glomerular capillaries as well (Figure 3C). Dilatation occurred not only for cortical distal nephron tubules but also for PTs that had a diminished brush border (Figure 3D).

In EGF-deficient mice, smooth muscle actin (SMA) immunolabeling (a marker of pericyte/myofibroblast activation) was increased in glomeruli and along crescents in Bowman's space, but extensive periglomerular SMA immunolabeling was observed as well (Figure 4A). The periglomerular and tubulointerstitial myofibroblast activation and fibrosis were associated with a strong influx of macrophages ($F4/80^{+}$) (Figure 4A). Glomerular IgG deposition and increased complement C3 lining glomerular capillaries were found as well (Figure 4B). Moreover, $CD45^{+}$ leukocytes and $CD3^{+}$ T-cells accumulated in glomeruli, as well as in periglomerular tissue and in tubulointerstitial areas (Figure 4C and 4D). No evidence for apoptotic degeneration was observed in these glomeruli (Figure 4D). These observations are consistent with findings seen in inflammatory crescentic glomerulonephritis.

As crescentic glomerulonephritis has been linked to aberrant hyperactivation of HB-EGF/EGFR signaling in glomeruli that does not occur in normal glomeruli (15), we assessed whether HB-EGF accumulation and EGFR activation occur in glomeruli of azotemic $Egf^{-/-}$ mice. Indeed, we found increased immunolabeling for HB-EGF in glomerular cells lining crescents along Bowman's capsule in azotemic $Egf^{-/-}$ mice (Figure 4E). Furthermore, we found in these mice strongly increased immunolabeling for phosphorylated EGFR (Tyr1068), which serves as a marker for increased EGFR signaling (Figure 4E). Thus, crescentic glomerulonephritis in $Egf^{-/-}$ mice that developed severe renal disease with renal failure is associated with hyperactivation of HB-EGF/EGFR signaling in glomeruli, similarly as reported for rapidly progressive glomerulonephritis in humans and mouse models (15). This suggests that physiological levels of EGF help protect the kidney from the development of glomerulonephritis.

Labeling kidneys with fluorescently-conjugated phalloidin and Lotus Tetragonolobus Lectin (LTL), which both visualize the apical brush border membrane of PTs, showed that EGF-deficient kidneys that had a highly increased BUN also had dilated PTs with an attenuated brush border (Figure 5A). Consistent with these findings, Western blotting using whole kidney lysates showed diminished protein levels of the PT marker Slc3a1 in $Egf^{-/-}$ mice that had severe renal impairment, whereas Slc3a1 protein levels were normal in aged $Egf^{-/-}$ mice with mild azotemia (Figure 2).

Immunolabeling for TAL, DCT, and CT/CD markers, showed that dilated distal nephron segments in the renal cortex of EGF-deficient mice that had significant renal impairment were mainly DCTs (NCC^+ and $Pvalb^+$) and CTs/cortical CDs ($Aqp2^+$), whereas TALs ($NKCC2^+$) were not dilated and their NKCC2 protein levels were not diminished (Figures 2 and 6). The observed morphologic DCT abnormalities were also accompanied by diminished protein levels of the DCT differentiation marker NCC in $Egf^{-/-}$ mice with high azotemia, but not in aged $Egf^{-/-}$ mice with no high increase in BUN (Figure 2). In contrast, none of these changes were observed in WT or TGFα-deficient mice.

We have previously observed in KCTD1-deficient mice that impaired DCT differentiation is followed by progressive renal fibrosis in these mice and is at least in part a consequence of β-catenin hyperactivation, which leads to an increase in phosphorylation of the mTOR targets 4E-BP1 and p70 S6K (2). Similarly, we find in those $Egf^{-/-}$ kidneys with significant renal fibrosis that loss of NCC is associated with increased renal active β-catenin levels and activation of mTOR signaling targets with increased phosphorylation of 4E-BP1 (Thr37/46) and p70 S6K (Figure 2). mTOR hyperactivation also sequesters the transcription factor TFEB to the cytoplasm (22), and we found increased cytoplasmic TFEB in dilated distal nephron segments in these $Egf^{-/-}$ kidneys as well (Figures 2 and 5B). In contrast, β-catenin/mTOR hyperactivation does not occur in aged $Egf^{-/-}$ mice that do not have renal fibrosis and renal failure (Figure 2). This suggests that EGF deficiency leads in a subset of mice to a state of impaired epithelial differentiation of specific nephron segments that promotes this severe kidney phenotype with glomerulonephritis, fibrosis, and inflammation.

DISCUSSION

Clinical data in patients with CKD suggests a link between reduced urinary EGF and CKD (8, 11). Moreover, exogenously administered EGF had a protective effect on renal functions in various mouse models with experimental impairment of kidney function, such as in a model of ischemia-reperfusion injury (20) or in a mouse model of autosomal recessive polycystic kidney disease (21). This suggests an important role of physiological EGF levels for the maintenance of renal homeostasis and kidney function in the adult.

To test whether physiological levels of EGF indeed support kidney health in the adult, we assessed the effects of genetic inactivation of EGF on renal function. Based on the observation of a genetic background-dependent large variability in the severity of phenotypes observed in mice lacking the EGF receptor (16), we speculated that EGF deficiency may also result in renal abnormalities that show significant variability in disease severity.

Indeed, our findings demonstrate that adult $Egf^{-/-}$ mice develop urinary microalbuminuria in the majority of mice (>50%), but only a subset of EGF-deficient mice develop more severe renal abnormalities that lead to a high increase in BUN and to major histopathological renal defects. This variability in the phenotype is unlikely explained by a random outlier effect, as none of the mice in the large control groups (neither WT nor $Tgfa^{-/-}$ mice) had a highly abnormal increase in BUN. Instead, the variability in the manifestation of renal pathologies in EGF-deficient mice suggests that EGF is a contributing but not essential factor to maintaining kidney health in the adult mammalian kidney.

As $Egf^{-/-}$ mice and $Egf^{-/-}Tgfa^{-/WT}$ mice have a mixed genetic background, this suggests that strain-specific genetic modifier alleles that segregate independently have a significant contribution to the severity of the observed kidney phenotype, but only when EGF is absent. WT and $Tgfa^{-/-}$ mice were generated from the same $Egf^{-/WT}Tgfa^{-/WT}$ offspring as $Egf^{-/-}$ mice and, therefore, they share also this mixed genetic background. As age-matched WT and $Tgfa^{-/-}$ experimental groups did not develop renal abnormalities, this suggests that in the presence of strain-specific genetic modifier alleles EGF plays a role in protecting the kidney from inflammation and fibrosis and in maintaining the structural integrity of glomeruli, PTs, and DCTs in the adult. Only when EGF is absent do renal abnormalities occur, consistent with the hypothesis that EGF deficiency is the rate-limiting determinant for the manifestation of glomerulonephritis, renal fibrosis, and inflammation in these mice.

A broad variability in the severity of renal abnormalities, as seen in EGF-deficient mice, has also been reported for genetic diseases that affect the kidney, both in humans as well as mouse mutants. A striking example in the mouse where a broad phenotypic variability is dependent on the genetic background is the EGF receptor-deficient mouse mutant (16). Similarly, in humans, phenotypes associated with polycystic kidney disease are highly variable in their clinical manifestations and can range from neonatal death to an adequate function in the adult (23). Even intrafamilial variability can be extensive between family members that carry the identical germline mutation, indicating the important influence that genetic background and environmental factors have on the manifestation of these renal pathologies. For example, extreme kidney disease discordance was observed within families with autosomal-dominant polycystic kidney disease, regardless of the underlying mutated gene or mutation class (24). Thus, our observation that not all EGF-deficient mice develop major renal pathologies does not diminish the relevance of the findings of a potential protective role of EGF for the maintenance of kidney function and indicates an important role of genetic modifiers for the manifestation of renal pathologies when EGF is lacking.

Collectively, together with the prior observations that exogenously administered EGF promotes repair of injured tubules in mouse models and that low urinary EGF is linked to CKD development in humans, our data suggest that physiological levels of EGF have a protective role for the adult kidney. However, the findings also demonstrate that EGF is not an essential factor for normal kidney function, as not all aged $Egf^{-/-}$ mice developed severe kidney abnormalities. Instead, the manifestation of glomerulonephritis, renal fibrosis, and inflammation in a subset of EGF-deficient mice suggests that EGF acts as a promoter of protective functions and repair in the nephron in addition to other modifier genes whose

activities may be distinct between different mice explained by the heterogeneous genetic background.

Supplementary Material

Refer to Web version on PubMed Central for supplementary material.

ACKNOWLEDGMENTS:

The authors would like to thank Dr. Robert B. Colvin for critical discussions. This study was supported by funding from the NIH (R01DK118134, R01DK121178, R21AG063377) to AGM.

DATA AVAILABILITY STATEMENT:

The data that support the findings of this study are available in the methods and/or supplementary material of this article.

List of nonstandard abbreviations:

EGF	epidermal growth factor
EGFR	epidermal growth factor receptor
DCT	distal convoluted tubule
TAL	thick ascending limb of Henle
PT	proximal tubule
CT	connecting tubule
CD	collecting duct
LOH	Loop of Henle
CKD	chronic kidney disease
WT	wildtype
CTGF	connective tissue growth factor
P	postnatal day
BUN	blood urea nitrogen
HB-EGF	heparin-binding epidermal growth factor
TGFα	transforming growth factor α
ARRIVE	Animal Research: Reporting of In Vivo Experiments

REFERENCES

1. Raaberg L, Nexo E, Damsgaard Mikkelsen J, and Seier Poulsen S (1988) Immunohistochemical localisation and developmental aspects of epidermal growth factor in the rat. Histochemistry 89, 351–356 [PubMed: 3261722]
2. Marneros AG (2020) AP-2beta/KCTD1 Control Distal Nephron Differentiation and Protect against Renal Fibrosis. Dev Cell 54, 348–366 e345 [PubMed: 32553120]
3. Jung JY, Song JH, Li C, Yang CW, Kang TC, Won MH, Jeong YG, Han KH, Choi KB, Lee SH, and Kim J (2005) Expression of epidermal growth factor in the developing rat kidney. Am J Physiol Renal Physiol 288, F227–235 [PubMed: 15353402]
4. Groenestege WM, Thebault S, van der Wijst J, van den Berg D, Janssen R, Tejpar S, van den Heuvel LP, van Cutsem E, Hoenderop JG, Knoers NV, and Bindels RJ (2007) Impaired basolateral sorting of pro-EGF causes isolated recessive renal hypomagnesemia. J Clin Invest 117, 2260–2267 [PubMed: 17671655]
5. Luetteke NC, Qiu TH, Fenton SE, Troyer KL, Riedel RF, Chang A, and Lee DC (1999) Targeted inactivation of the EGF and amphiregulin genes reveals distinct roles for EGF receptor ligands in mouse mammary gland development. Development 126, 2739–2750 [PubMed: 10331984]
6. Callegari C, Laborde NP, Buenaflor G, Nascimento CG, Brasel JA, and Fisher DA (1988) The source of urinary epidermal growth factor in humans. Eur J Appl Physiol Occup Physiol 58, 26–31 [PubMed: 3264526]
7. Perheentupa J, Lakshmanan J, and Fisher DA (1985) Urine and kidney epidermal growth factor: ontogeny and sex difference in the mouse. Pediatr Res 19, 428–432 [PubMed: 3873640]
8. Ju W, Nair V, Smith S, Zhu L, Shedden K, Song PXK, Mariani LH, Eichinger FH, Berthier CC, Randolph A, Lai JY, Zhou Y, Hawkins JJ, Bitzer M, Sampson MG, Thier M, Solier C, Duran-Pacheco GC, Duchateau-Nguyen G, Essioux L, Schott B, Formentini I, Magnone MC, Bobadilla M, Cohen CD, Bagnasco SM, Barisoni L, Lv J, Zhang H, Wang HY, Brosius FC, Gadegbeku CA, Kretzler M, Ercb CPN, and Consortium PK-I (2015) Tissue transcriptome-driven identification of epidermal growth factor as a chronic kidney disease biomarker. Sci Transl Med 7, 316ra193
9. Chou JS, Reiser IW, and Porush JG (1997) Aging and urinary excretion of epidermal growth factor. Ann Clin Lab Sci 27, 116–122 [PubMed: 9098510]
10. Meybosch S, De Monie A, Anne C, Bruyndonckx L, Jurgens A, De Winter BY, Trouet D, and Ledeganck KJ (2019) Epidermal growth factor and its influencing variables in healthy children and adults. PLoS One 14, e0211212 [PubMed: 30677083]
11. Norvik JV, Harskamp LR, Nair V, Shedden K, Solbu MD, Eriksen BO, Kretzler M, Gansevoort RT, Ju W, and Melsom T (2020) Urinary excretion of epidermal growth factor and rapid loss of kidney function. Nephrol Dial Transplant
12. Ransick A, Lindstrom NO, Liu J, Zhu Q, Guo JJ, Alvarado GF, Kim AD, Black HG, Kim J, and McMahon AP (2019) Single-Cell Profiling Reveals Sex, Lineage, and Regional Diversity in the Mouse Kidney. Dev Cell 51, 399–413 e397 [PubMed: 31689386]
13. Staruschenko A, Palygin O, Ilatovskaya DV, and Pavlov TS (2013) Epidermal growth factors in the kidney and relationship to hypertension. Am J Physiol Renal Physiol 305, F12–20 [PubMed: 23637204]
14. Gesualdo L, Di Paolo S, Calabro A, Milani S, Maiorano E, Ranieri E, Pannarale G, and Schena FP (1996) Expression of epidermal growth factor and its receptor in normal and diseased human kidney: an immunohistochemical and in situ hybridization study. Kidney Int 49, 656–665 [PubMed: 8648906]
15. Bollee G, Flamant M, Schordan S, Fligny C, Rumpel E, Milon M, Schordan E, Sabaa N, Vandermeersch S, Galaup A, Rodenas A, Casal I, Sunnarborg SW, Salant DJ, Kopp JB, Threadgill DW, Quaggin SE, Dussaule JC, Germain S, Mesnard L, Endlich K, Boucheix C, Belenfant X, Callard P, Endlich N, and Tharaux PL (2011) Epidermal growth factor receptor promotes glomerular injury and renal failure in rapidly progressive crescentic glomerulonephritis. Nat Med 17, 1242–1250 [PubMed: 21946538]

16. Threadgill DW, Dlugosz AA, Hansen LA, Tennenbaum T, Lichti U, Yee D, LaMantia C, Mourton T, Herrup K, Harris RC, and et al. (1995) Targeted disruption of mouse EGF receptor: effect of genetic background on mutant phenotype. Science 269, 230–234 [PubMed: 7618084]

17. Marneros AG (2021) Magnesium and Calcium Homeostasis Depend on KCTD1 Function in the Distal Nephron. Cell Rep 34, 108616 [PubMed: 33440155]

18. Levchenko V, Zheleznova NN, Pavlov TS, Vandewalle A, Wilson PD, and Staruschenko A (2010) EGF and its related growth factors mediate sodium transport in mpkCCDc14 cells via ErbB2 (neu/HER-2) receptor. J Cell Physiol 223, 252–259 [PubMed: 20049896]

19. Pavlov TS, Levchenko V, O'Connor PM, Ilatovskaya DV, Palygin O, Mori T, Mattson DL, Sorokin A, Lombard JH, Cowley AW Jr., and Staruschenko A (2013) Deficiency of renal cortical EGF increases ENaC activity and contributes to salt-sensitive hypertension. J Am Soc Nephrol 24, 1053–1062 [PubMed: 23599382]

20. Humes HD, Cieslinski DA, Coimbra TM, Messana JM, and Galvao C (1989) Epidermal growth factor enhances renal tubule cell regeneration and repair and accelerates the recovery of renal function in postischemic acute renal failure. J Clin Invest 84, 1757–1761 [PubMed: 2592559]

21. Gattone VH 2nd, Lowden DA, and Cowley BD Jr. (1995) Epidermal growth factor ameliorates autosomal recessive polycystic kidney disease in mice. Dev Biol 169, 504–510 [PubMed: 7781894]

22. Napolitano G, Di Malta C, Esposito A, de Araujo MEG, Pece S, Bertalot G, Matarese M, Benedetti V, Zampelli A, Stasyk T, Siciliano D, Venuta A, Cesana M, Vilardo C, Nusco E, Monfregola J, Calcagni A, Di Fiore PP, Huber LA, and Ballabio A (2020) A substrate-specific mTORC1 pathway underlies Birt-Hogg-Dube syndrome. Nature 585, 597–602 [PubMed: 32612235]

23. Rossetti S, and Harris PC (2007) Genotype-phenotype correlations in autosomal dominant and autosomal recessive polycystic kidney disease. J Am Soc Nephrol 18, 1374–1380 [PubMed: 17429049]

24. Lanktree MB, Guiard E, Li W, Akbari P, Haghighi A, Iliuta IA, Shi B, Chen C, He N, Song X, Margetts PJ, Ingram AJ, Khalili K, Paterson AD, and Pei Y (2019) Intrafamilial Variability of ADPKD. Kidney Int Rep 4, 995–1003 [PubMed: 31317121]

A

Egf$^{-/-}$ (-/+ x -/+) [n=32 offspring]; observed % (expected %)			
-/-	-/+	+/+	
8	15	9	
25% (25%)	46.9% (50%)	28.1% (25%)	
Tgfa$^{-/-}$ (-/+ x -/-) [n=61 offspring]; observed % (expected %)			
-/-	-/+		
28	33		
45.9% (50%)	54.1% (50%)		

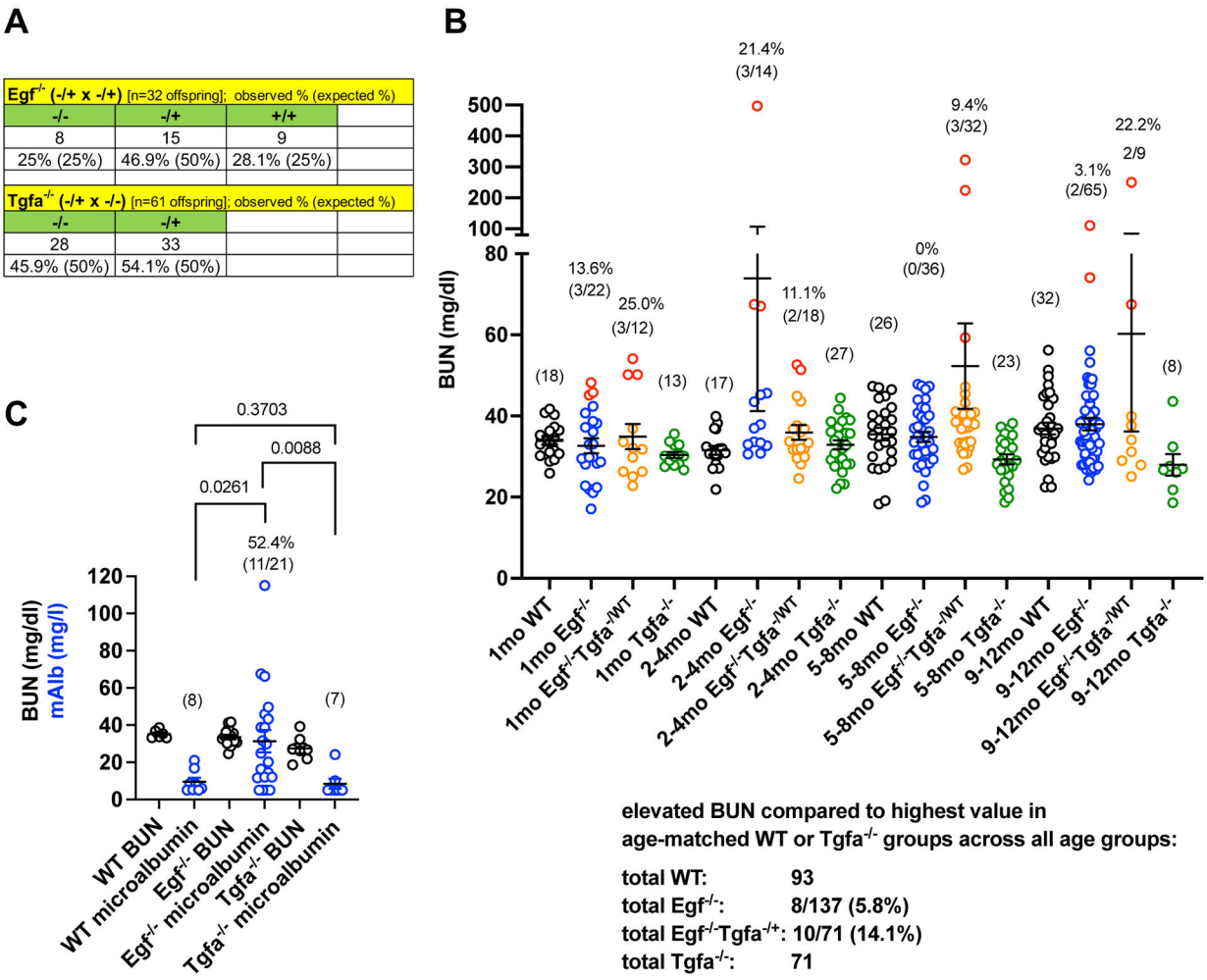

Figure 1: EGF deficiency leads to highly increased BUN levels in a subset of adult mice.

A. Mendelian ratios in 4-weeks old offspring from indicated crosses. Absolute numbers and percentiles are shown. Parentheses show expected Mendelian ratios. The deficiency of *Egf* or *Tgfa* does not affect the viability of these mice.

B. BUN serum levels were measured in different age groups (up to 12 months of age) in WT, Egf$^{-/-}$ mice, Egf$^{-/-}$Tgfa$^{-/WT}$ mice, and Tgfa$^{-/-}$ mice derived from the same intercrosses of Egf$^{-/WT}$Tgfa$^{-/WT}$ mice. Every measurement represents a different mouse (not serial measurements on the same mice). A subset of Egf$^{-/-}$ mice and Egf$^{-/-}$Tgfa$^{-/WT}$ mice show increased BUN levels relative to their age-matched WT or Tgfa$^{-/-}$ control mice (circles with red margin). BUN levels in Tgfa$^{-/-}$ mice were within the same normal range as seen in WT mice. An increased BUN value was defined as being higher than the highest BUN value in the age-matched WT and Tgfa$^{-/-}$ group. For each column of Egf$^{-/-}$ mice and Egf$^{-/-}$Tgfa$^{-/WT}$ mice, the percentile of mice with an increased BUN is shown (%), as well as the total numbers of mice with an increased BUN of the total numbers of mice in that group (number of mice with increased BUN/total number of mice). Graph shows mean ± SEM. Below the graph, the summary indicates for Egf$^{-/-}$ mice and Egf$^{-/-}$Tgfa$^{-/WT}$ mice across all age groups the percentile and the total number of mice with an increased BUN relative to the total number of mice of these groups.

C. Graph shows BUN values (mg/dl) in black and urinary microalbumin concentrations (mAlb in mg/l) in blue. For the $Egf^{-/-}$ mouse group the percentile of mice with increased urinary microalbumin is shown (%), as well as the total numbers of mice with increased urinary microalbumin of the total numbers of mice in that group (number of mice with increased urinary microalbumin/total number of mice). An increased value was defined to be higher than the highest value in the WT and $Tgfa^{-/-}$ group. A relative increase in urinary microalbumin is present in $Egf^{-/-}$ mice with normal BUN serum levels. Age-matched $Tgfa^{-/-}$ mice derived from the same intercrosses do not show increased urinary microalbumin compared to WT controls. All mice are ~10–13 months of age. P-values are shown for microalbumin measurements compared to the WT group (Mann-Whitney test). Graph shows mean ± SEM.

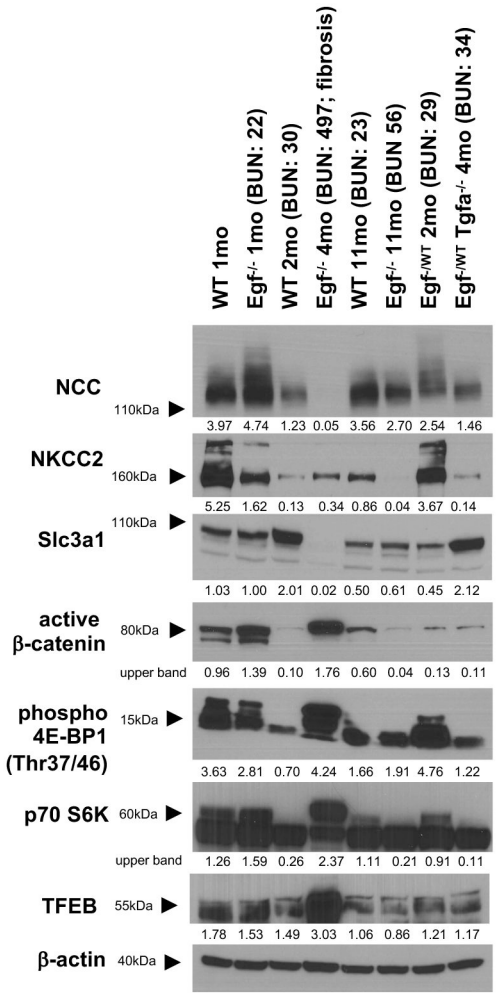

Figure 2: Azotemic EGF-deficient mice show loss of DCT and PT differentiation markers and increased renal β-catenin/mTOR signaling activity.

Western blotting of whole kidney lysates from the following mice: WT mice with normal kidney function (1-, 2- and 11-months-old), 1 months-old $Egf^{-/-}$ mice with normal kidney function, 4 months-old $Egf^{-/-}$ mouse with renal failure and fibrosis (BUN 497; shown in Figures 2 and 3), 11-months-old $Egf^{-/-}$ mouse with a moderate increase in BUN (56) and no renal fibrosis, 2-months-old $Egf^{-/WT}$ mouse (BUN 29) and 4-months-old $Egf^{-/WT}Tgfa^{-/-}$ mouse with normal kidney function (BUN 34). The 4 months-old $Egf^{-/-}$ mouse kidney with renal failure and fibrosis shows diminished protein levels of NCC and Slc3a1 (but not of NKCC2), increased active β-catenin levels and mTOR activation, with an increase in phosphorylation of 4E-BP1 at Thr37/46, p70 S6 kinase and TFEB. In contrast, the kidney of the 11-months-old $Egf^{-/-}$ mouse with a moderate increase in BUN (56) and no renal fibrosis did not show these changes. Black arrowheads indicate protein size (based on protein ladder, indicated in kDa). Values show densitometric values for Western blot bands normalized to β-actin.

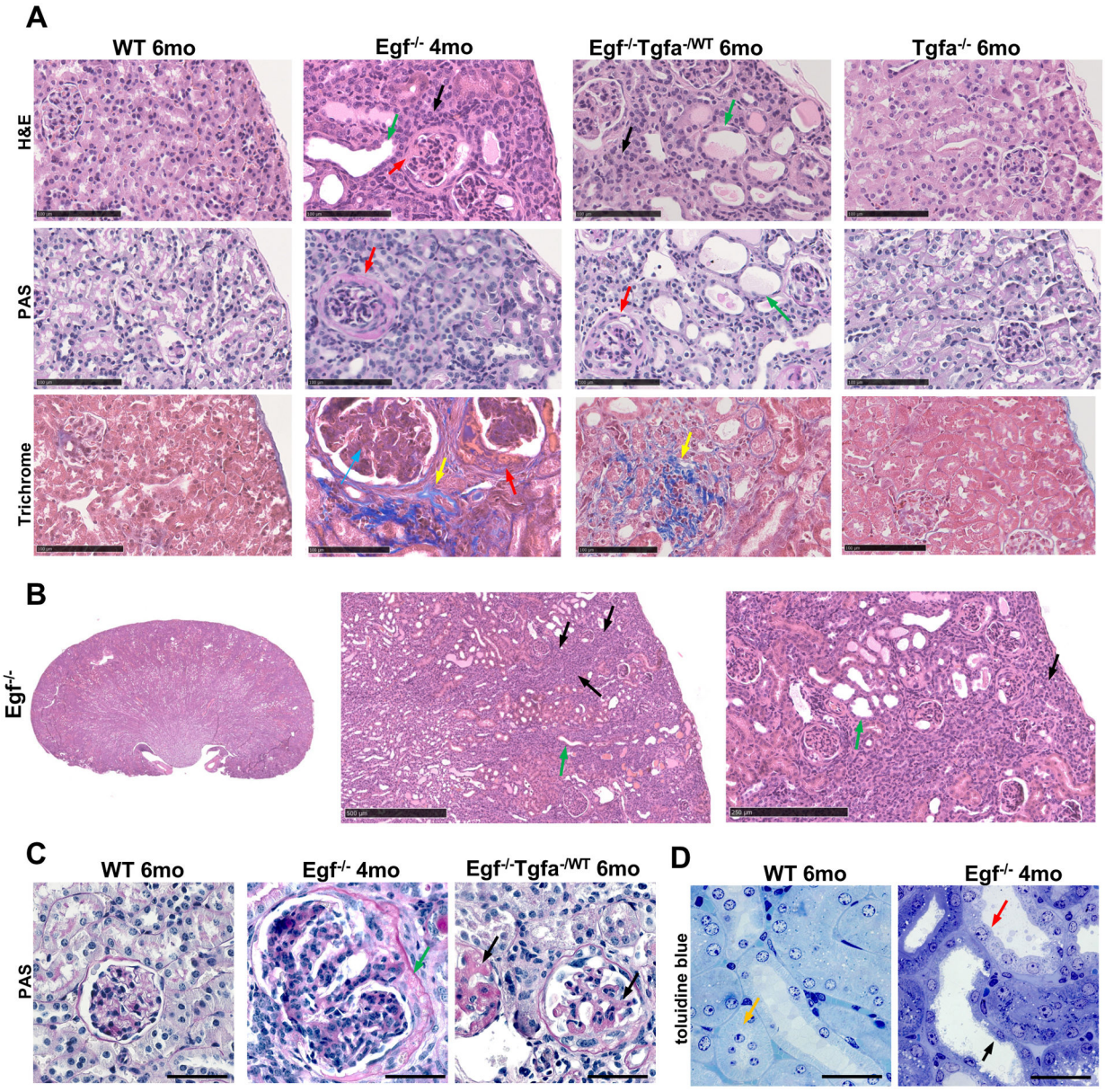

Figure 3: Crescentic glomerulonephritis, renal fibrosis, and dilatation of PTs and distal nephron segments in azotemic Egf$^{-/-}$ mice.

A. H&E, PAS, and Trichrome stained kidney sections from a 6-months-old WT mouse, a 4-months-old Egf$^{-/-}$ mouse with renal failure (BUN 497), a 6-months-old Egf$^{-/-}$Tgfa$^{-/WT}$ mouse with renal failure (BUN 224), and a 6-months-old Tgfa$^{-/-}$ mouse that has normal kidney function (BUN 19). Lack of EGF leads to dilatation of distal nephron segments in the renal cortex with protein casts (green arrows), as well as atrophic tubular structures with a diminished lumen (black arrows) in Egf$^{-/-}$ and Egf$^{-/-}$Tgfa$^{-/WT}$ mice. Glomeruli in kidneys of azotemic Egf$^{-/-}$ mice or Egf$^{-/-}$Tgfa$^{-/WT}$ mice show cellular crescents in Bowman's space (red arrows). Trichrome staining shows areas of tubulointerstitial cortical fibrosis (blue; yellow arrows) and glomerulosclerosis (blue; blue arrow) in Egf$^{-/-}$ and Egf$^{-/-}$Tgfa$^{-/WT}$ mice as well. These changes are not seen in WT or Tgfa$^{-/-}$ mice. Scale bars 100 μm.

B. Lower magnification H&E images of same $Egf^{-/-}$ mouse kidney as shown in (A). Wedge-shaped cortical areas with atrophic tubules that have a diminished lumen are seen (black arrows), as well as dilated tubular segments (green arrow). Scale bar 500 μm (middle) and 250 μm (right).

C. Higher magnification images of glomeruli of kidneys stained with PAS of WT, $Egf^{-/-}$ and $Egf^{-/-}Tgfa^{-/WT}$ mice shown in (A). EGF deficiency is associated with lobulated glomeruli and the formation of cellular crescents in Bowman's space (green arrow). PAS^{+} material is also seen in glomerular capillaries in these mice (black arrows). Scale bars 50 μm.

D. Toluidine blue staining of semithin plastic-embedded kidneys of WT mice and $Egf^{-/-}$ mice with azotemia. Dilated distal nephron tubules are seen in $Egf^{-/-}$ mice (red arrow). PTs show dilatation and a diminished apical brush border membrane in $Egf^{-/-}$ mice as well (black arrow), which is not seen in WT littermates (orange arrow). Scale bars 50 μm.

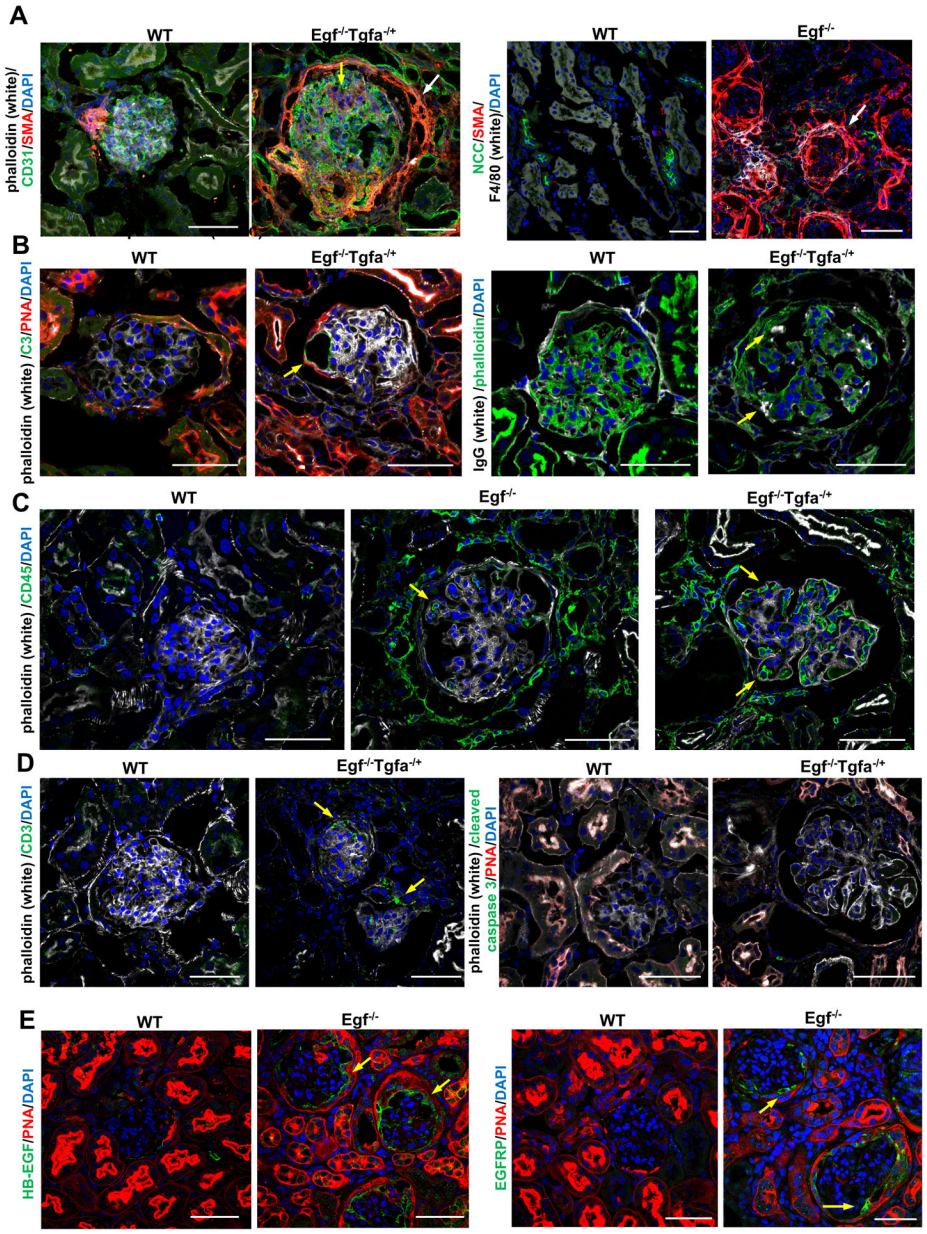

Figure 4: Crescentic glomerulonephritis associated with HB-EGF/EGFR hyperactivation in azotemic EGF-deficient mice.

A. Left: Co-immunolabeling for smooth muscle actin (SMA) and the endothelial cell marker CD31 (left panel) shows glomerulosclerosis (yellow arrow) and cellular crescents with strongly SMA^{+} parietal Bowman's capsule in azotemic $Egf^{-/-}Tgfa^{-/WT}$ mice (white arrow). Bowman's capsule does not show SMA immunoreactivity in age-matched WT mice. Right: $F4/80^{+}$ macrophages strongly accumulate at sites of periglomerular fibrosis and the tubulointerstitial space in these mice as well, whereas this macrophage accumulation is not seen in the kidneys of WT mice (NCC in green labels DCTs).

B. Left: C3 immunolabeling (green; yellow arrow) is detected in dilated glomerular capillaries in azotemic $Egf^{-/-}Tgfa^{-/WT}$ mice but not in WT mice. Right: Glomerular IgG deposits (yellow arrows) are seen in azotemic $Egf^{-/-}Tgfa^{-/WT}$ mice.

C. CD45 immunolabeling shows an extensive leukocytic cellular infiltrate in the tubulointerstitial space, the periglomerular area and also within glomeruli in azotemic $Egf^{-/-}$ mice and $Egf^{-/-}Tgfa^{-/WT}$ mice but not in WT controls (yellow arrows).
D. Left: $CD3^{+}$ T-cells (yellow arrows) are seen in glomeruli of azotemic $Egf^{-/-}Tgfa^{-/WT}$ mice but not in glomeruli of WT mice. Right: No cleaved caspase 3^{+} cells (apoptosis marker) are observed in glomeruli of WT or $Egf^{-/-}Tgfa^{-/WT}$ mice.
E. Left: HB-EGF immunolabeling shows increased HB-EGF in glomerular cells adjacent to crescents (yellow arrows) in EGF-deficient mice. Right: An antibody against phosphorylated EGFR (Tyr1068) that is associated with activation of EGFR signaling activity shows strongly increased EGFR activation in crescents of glomeruli in EGF-deficient mice (yellow arrows). WT controls do not show this increase in HB-EGF and EGFR (Tyr1068) phosphorylation.
Scale bars 50 μm. Kidney sections from a 6-months-old WT mouse, a 4-months-old $Egf^{-/-}$ mouse with renal failure (BUN 497), and a 6-months-old $Egf^{-/-}Tgfa^{-/WT}$ mouse with renal failure (BUN 224), as shown in Figure 2.

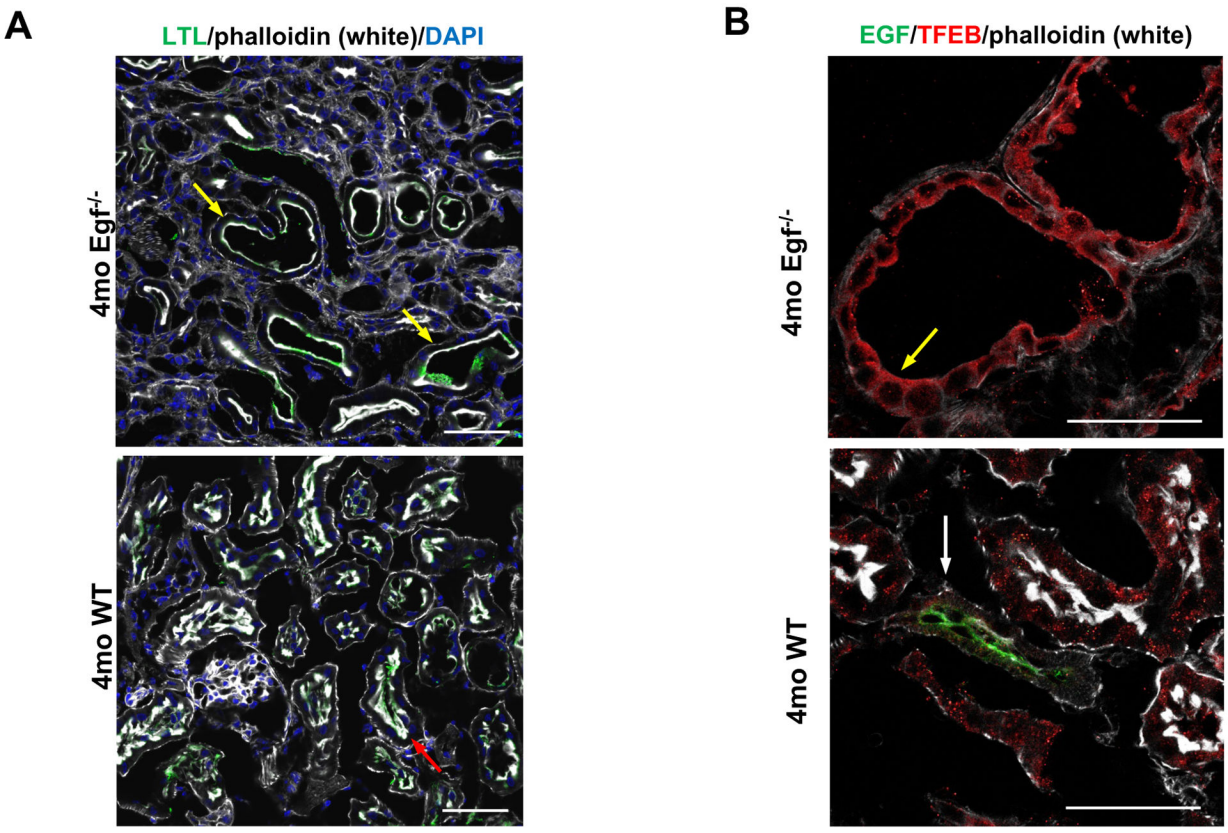

Figure 5: EGF-deficient mice with renal insufficiency show PT and DCT defects.

A. Lotus Tetragonolobus Lectin (LTL, in green) and phalloidin (in white) label the apical brush border membrane of PTs (red arrow). Dilatation of PTs and an attenuation of the brush border membrane are observed in azotemic EGF-deficient mice (yellow arrows). Scale bars 50 μm.

B. Immunolabeling of the 4 months-old $Egf^{-/-}$ mouse kidney with renal failure and fibrosis (shown in A and B) demonstrates increased cytoplasmic TFEB labeling in distal nephron segments (yellow arrow) compared to EGF-expressing distal nephron segments (white arrow) in WT littermates. Scale bars 50 μm.

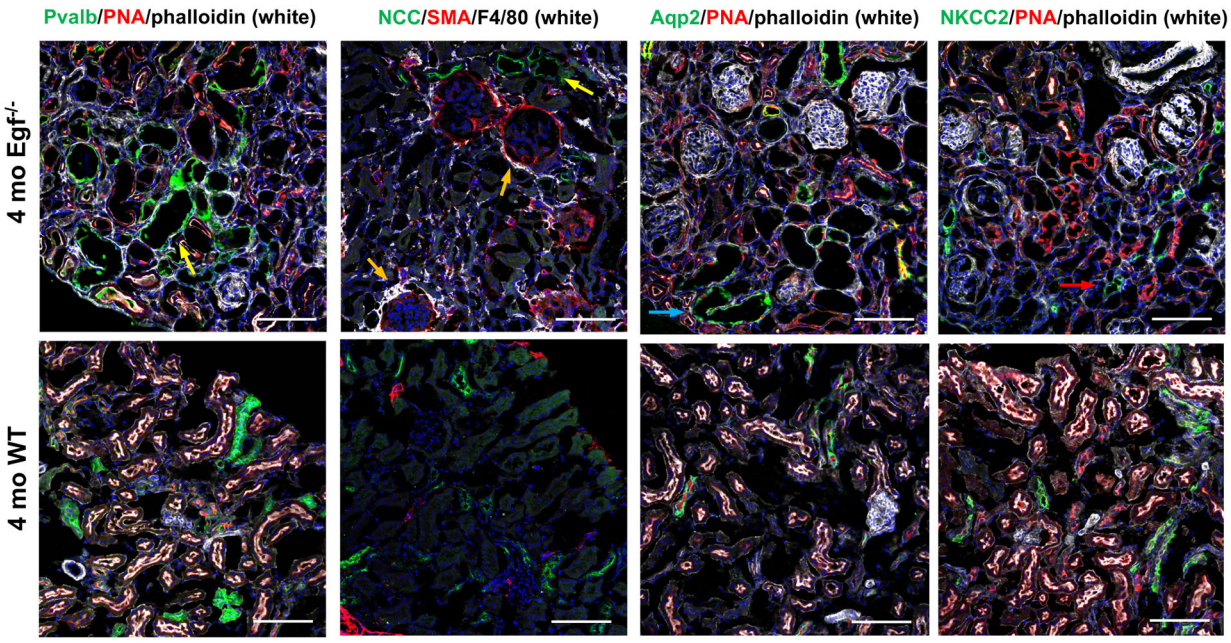

Figure 6: EGF-deficient mice with renal insufficiency show dilatation of DCTs and CTs and periglomerular fibrosis.

Immunolabeling of a 4 months-old $Egf^{-/-}$ mouse kidney with renal failure and fibrosis shows dilated DCTs ($Pvalb^{+}NCC^{+}$) (yellow arrows) and CTs/cortical CDs ($Aqp2^{+}$) (blue arrow), increased macrophage infiltration ($F4/80^{+}$), and fibrosis with SMA^{+} myofibroblasts particularly in a periglomerular distribution (orange arrows), whereas TALs ($NKCC2^{+}$) are not dilated (red arrow). These changes are not seen in a WT age-matched littermate. PNA (rhodamine-conjugated peanut agglutinin) labels distal nephron epithelial cells, whereas contiguous red labeling is seen in PTs. Scale bars 100 μm.